1003-7713/2002/03-218-6

(VUV + UV)-REMPI Detection of the Methyl Radical Product in a Crossed-beam Scattering Experiment *

Teh Waileong[a], Shiu Weicheng, Zhou Jingang, Liu Kopin[b]
(*Institute of Atomic and Molecular Sciences, Academia Sinica P. O. Box* 23-166, *Taipei* 106)

Abstract A (VUV + UV)-REMPI spectroscopy scheme was exploited to detect the methyl radical (CH_3). To demonstrate its high sensitivity, a crossed-beam scattering experiment was conducted with CH_3 (CD_3) as the reaction product from F + CH_4 (CD_4). The absolute detection limit was estimated to be about $10^7/cm^3$. From the observed spectra, the spectroscopic constants of the two intermediate Rydberg states, 3d $^2E''$ and 3d $^2A_1'$, were also refined.

Key words Four-wave mixing, Resonance-enhanced multiphoton ionization (REMPI), Rydberg state, Methyl
CLC number: O64 **Document**: A

1 Introduction

Fundamentally, the methyl radical (CH_3) stands at a unique position as a prototype for the entire class of alkyl radicals. Practically, it is an important species in the early stages of hydrocarbon combustion[1], in the chemistry of the troposphere[2], and is believed to play a key role in the growth of thin film diamond by chemical vapor deposition (CVD) methods[3]. Because of both its fundamental importance and the practical needs, the methyl radical has been the subject of numerous experimental[4-15] and theoretical studies[16-18]. In particular, there have been extensive research efforts focused on the development of various sensitive and selective detection methods for diagnostic purposes[4-12]. Among them, the resonance-enhanced multiphoton ionization (REMPI) spectroscopy, either the (2 + 1) or (3 + 1) REMPI scheme[7-10], is certainly a viable one and has enjoyed a wide range of applications. In a recent review, it has in fact been stated[19] that "of all the radicals so far detected by REMPI spectroscopy, it is probably the newly identified multiphoton resonances of the methyl radical that have had the greatest impact outside the spectroscopic community".

In this contribution, an alternative, (VUV + UV)-REMPI detection scheme will be presented. The ground state of CH_3 is of $^2A_2''$ symmetry in D_{3h} geometry. Most of known, electronically excited states of CH_3 are of predissociative Rydberg states[4,16-18]. The predisssociation lifetime is typically in the order of ps[15], which renders the laser-induced fluorescence a sensible detection method. The intermediate states we used are the $^2E''$ and the $^2A_1'$ states, via the so-called γ_1 ($2p \rightarrow 3d$, $\tilde{X}^2A_2'' \rightarrow {}^2E''$) and δ_1 ($2p \rightarrow 3d$, $\tilde{X}^2A_2'' \rightarrow {}^2A_1'$) transitions, respectively. These two electronic transitions have previously been characterized by Herzberg[4].

To demonstrate that the proposed (VUV + UV)-REMPI detection scheme is a promising alternative with sufficient sensitivity in many applications, a crossed-beam experiment on F + $CH_4/CD_4 \rightarrow$ HF/DF + CH_3/CD_3 was performed. To aid in further spec-

* To whom correspondence should be addressed, E-mail: kpliu@gate.sinica.edu.tw. a. Present address: Department of Planetary Science, National Central University, Chung-Li, Taiwan 32054; b. Also Department of Chemistry, National Taiwan University, Taipei 106.

Received date: 2002-03-07.

troscopic characterization of the observed γ_1- and δ_1-bands, a single beam experiment with a supersonically cooled CH_3 or CD_3 radical was also conducted. In this report, we will focus on the spectroscopic aspects of this detection scheme, rather than the reaction dynamics. The paper is organized as follows. The next section describes the experimental details, particularly for the generation of the tunable VUV radiation. The (1 + 1′) REMPI spectra of CH_3 and CD_3, from both crossed-beam scattering and the radical beam, are then presented and analyzed. The last section summarizes the pros and cons of this detection scheme.

2 Experiment

The experiments were conducted with the crossed-beam apparatus described in details previously[20-22]. In brief, for the scattering experiment a discharge source was used to generate the F-atom beam. For the single-beam experiment, the same discharge source, but with CH_4 or CD_4 (10% seeded in He at 505 kPa) as the precusor, produced the supersonically cooled CH_3 or CD_3 radical.

The methyl radical was interrogated by the (VUV + UV)-REMPI spectroscopy coupled with a time-of-flight (TOF) mass spectrometer[20]. The usual boxcar integrator was used in data acquisition with the gate set at $m/e = 15$ or 18 for CH_3 or CD_3, respectively. The desired VUV radiation (66000-68000 cm^{-1}) was generated by a two-photon resonant, difference-frequency mixing technique in xenon[23]. Fig.1 shows the four-wave mixing scheme and the relevant energy level diagram of xenon. Fig.2 depicts the experimental setup. A YAG laser pumped two dye lasers simultaneously. The wavelength of ω_1 was fixed at 499.252 nm, whose frequency-doubled output was two-photon resonant with Xe $6p[1/2]_0$ state. The wavelength of ω_2 was tunable, centering around 742 nm, The laser energies were typically 1.5 and 5 mJ/pulse for $2\omega_1$ and ω_2, respectively. The VUV cell consists of two lenses. An achromatic doublet ($f = 15$ cm) serves as the input window, while a LiF lens ($f = 7.5$ cm) as the output. This arrangement resulted in a parallel VUV laser (near 150 nm) and a diverging (residual) input UV/visible lasers.

The VUV laser was generated via a four-wave difference-frequency mixing process, $\omega_{VUV} = 2\omega_1 - \omega_2$ in Xe (see Fig.1). The phase-matched pressure was found to be 533666 Pa. Also shown in Fig.1 (the dashed lines) is a sum-frequency mixing process (for which Xe is a negative dispersion medium) that could compete with the desired 150 nm generation. This deep VUV wavelength is just beyond the transmission cutoff of the LiF lens, thus its radiation never reaches our detector to monitor the VUV intensity. Nevertheless, experimental evidence for its existence will be presented in the next section.

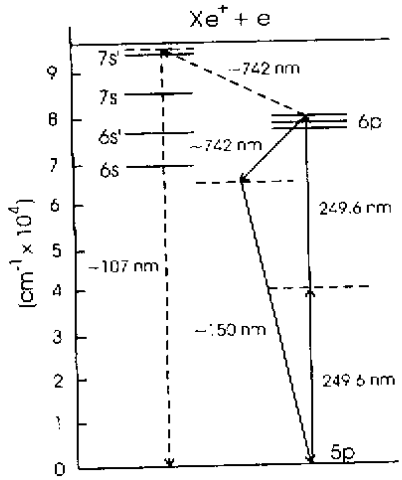

Fig.1 Energy level diagram of xenon
The two-photon resonant state is Xe $5p^5 6p[1/2]_0$. The difference-frequency mixing process (the solid lines) generates the desired VUV radiation at 150 nm, whereas the sum-frequency process (the dashed lines) competes with the desired process.

To further enhance the VUV output for a higher sensitivity, a few tasks were undertaken. As seen from Fig.2, a telescope was inserted in the 740 nm (ω_2) beam for better match of the confocal parameters of the two input lasers. Second, a $\lambda/4$-waveplate was used to change the polarization of the UV ($2\omega_1$) input laser into a circular one to eliminate, by the conservation of angular momentum, the competing frequency-tripling process ($3\omega_1$) in Xe. Finally, a time-delay of ω_2 and $2\omega_1$ was set such that ω_2 proceeded $2\omega_1$ by about (0.4 ± 0.1) ns (both laser pulses with a FWHM of 2 ns). Together, these three measures resulted in an increase of the VUV intensity, so as the REMPI

signal, by a factor of 6.

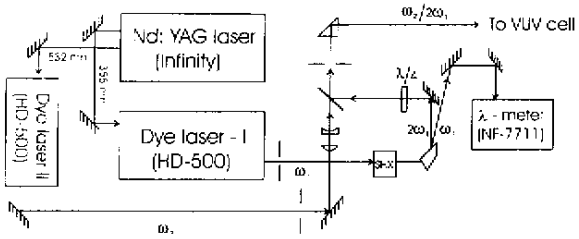

Fig.2 Optical layout for the VUV generation
The wavelength of ω_1 is fixed at 499.252 nm, and that of ω_2 is tunable. SHX denotes a second harmonic crystal (BBO).

3 Results

Fig.3 shows a series of (VUV + UV)-REMPI spectra of the CH_3 radical. The upper ones correspond to the CH_3 products from the F + CH_4 reaction at 5 different collision energies. The lowest one is the spectrum taken with the discharge-generated CH_3 beam. Most of the gross features in this wavelength region can readily be identified and labeled, according to the Herzberg's assignments[4], as the vibronic transitions of either the γ_1 or δ_1 Rydberg series. The modern-day notation, e.g., "2_3^1" indicating the hot band transition of the ν_2 vibrational mode (the umbrella mode) with three (and one) quanta excitation in the electronically ground (and excited) state, is adapted here. And the "0_0^0" band indicates the transition between the ground vibrational states of the upper and lower electronic states. Similar results for the CD_3 case are shown in Fig.4.

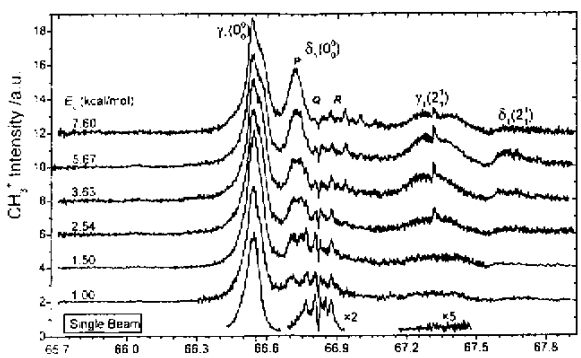

Fig.3 (VUV + UV)-REMPI spectra of the CH_3 from the F + CH_4 reaction and from a discharge source (the bottom one)
The vibronic assignment is indicated. The vertical dotted line denotes the ν_0 position from the rotational analysis.

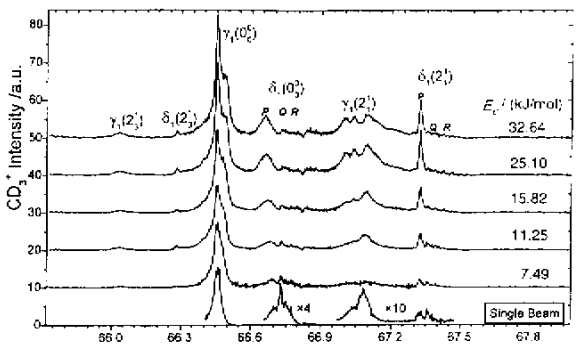

Fig.4 As Fig.3, except for CD_3

A few band-assignments deserve special attention. First, the P-head of the $\delta_1(0_0^0)$ transition which occurs at 66720 cm^{-1} for CH_3 and 66660 cm^{-1} for CD_3, is quite prounanced for crossed beam results at higher collision energies but is nearly absent in the case of single beam. This can be reconciled after the rotational analysis of the Q- and R-branches of this vibronic band. Fig. 5 enlarges portions of spectral regions for illustration via the rotational analysis. The $\delta_1(0_0^0)$ band is a $^2A_2'' \rightarrow {}^2A_1'$ transition (a //-type). The rotational selection rules are: $\Delta K = 0$; $\Delta N = \pm 1$ for $K = 0$, and $\Delta N = 0, \pm 1$ for $K \neq 0$[24]. The N is the quantum number describing rotation of the nuclei (excluding spin), K is the projection of N on the molecular axis. In addition, for a planar, symmetric-top molecule with identical nuclei the symmetry of the rotational wavefunction dictates the nuclear spin statistics. In the case of $CH_3(CD_3)$, the statistical factor is 2(11) for $N = 0,3,6,\cdots$; and 1(8) for all other N's. In addition, for $K = 0$, it is 4(1) and 0(10) for even and odd N, respectively. Hence, the observed even and odd alternation in intensities shown in Fig.35, i.e., favoring even N for CH_3 and odd N for CD_3, for the crossed-beam data suggests immediately the dominance of the product population in the $K = 0$ stack of energy levels. This is in contrast to the single-beam data, where no such an even-odd alternation was observed because a cold and thermal (N, K)-distribu-

tion is more likely. Note that the observation of a much weaker Q-head (recalling the selection rule of $\Delta N = \pm 1$ for $K = 0$) in the crossed-beam spectrum than that from the single beam data is also consistent with this interpretation. The implication to reaction dynamics will be discussed in a future publication.

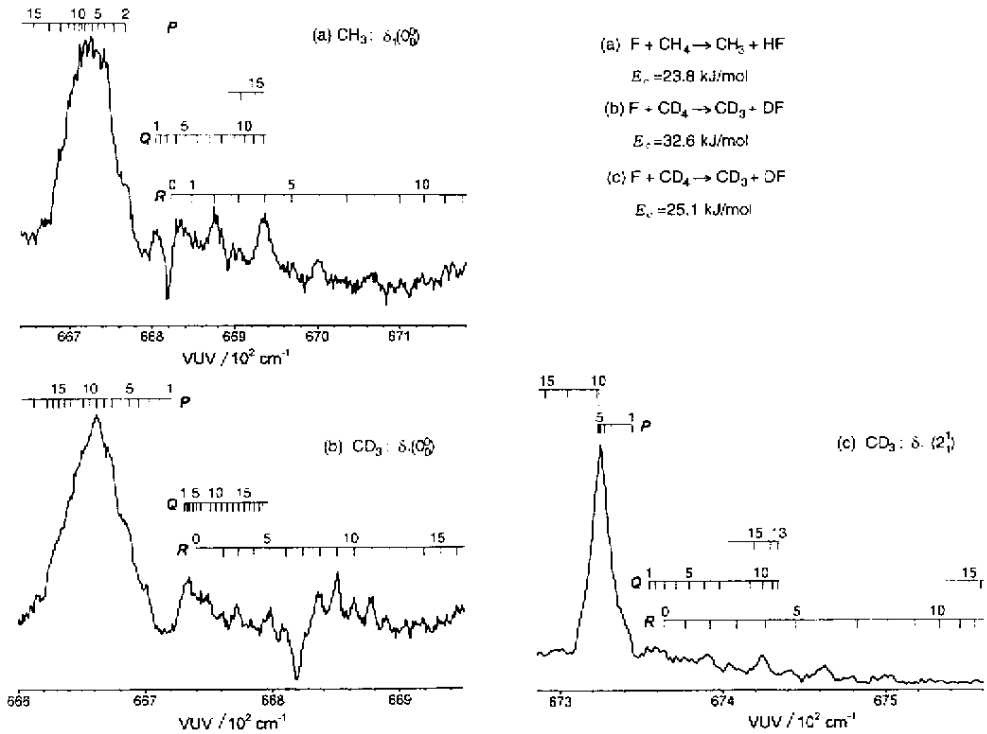

Fig.5 Enlarged scale of the $\delta_1(0_0^0)$ bands and the $\delta_1(2_1^1)$ band (for CD_3) for the rotational analysis
See text for details about the origin of the "dip" near 66820 cm^{-1}.

Because of the dominance of $K = 0$ levels and the lack of the K sub-band structure (presumably from the lifetime broadening), the energy positions of the observed R-branch transitions of the spectra shown in Fig.5 are then fitted with a simplified (i.e., neglecting the K-dependency) form

$$\nu = \nu_0 + B'N'(N'+1) - B''N''(N''+1) - D'N'^2(N'+1)^2 + D''N''^2(N''+1)^2$$

In this equation ν_0 is the origin of the $\delta_1(0_0^0)$ vibronic band, B'' (B') and D'' (D') are the rotational and centrifugal distortion constants of the ground (excited) state. We used the literature values of B'' and D'' by Hirota and co-workers for CH_3[11,12] and those by Sears *et al.* for CD_3[5,6] in our fit. The resulted ν_0, B', and D' constants are listed in Table 1, along with the Herzberg's results for comparison. The general agreement is good. More importantly, this rotational analysis led to the ready assignment of the P-head for the aforementioned, prominent peak. Similar analysis was performed for the $\delta_1(2_1^1)$ band in the case of CD_3, see Fig.5 and Table 1. Once again, a pronounced even-odd alternation in peak intensities is noted. Contrary to the ground vibronic band $\delta_1(0_0^0)$ of CD_3, the even N

Table 1 Molecular parameters (in cm^{-1}) of methyl radical derived from the fitting of $\delta_1(0_0^0)$ and $\delta_1(2_1^1)$ bands. Values in parentheses denote one standard deviation, given in units of the last digit from a least-squares fit.

	CD_3		CH_3	
$\nu_2' = 0$ B_v	5.064(1)	5.137[4]	11.00(1)	10.72[4]
10^4 D_N	4.49(3)	10[4]	4.6(3)	
$\nu_2' = 1$ B_v	5.676(3)			
10^4 D_N	30.4(3)			
$\nu_0(0_0^0)$	66728.67(3)	66723.1[4]	66800.1(3)	66799.4[4]
$\nu_0(2_1^1)$	67352.56(5)	67323.2P[4]		
		67355.1Qh[4]		
$\nu_0(2_3^1)$	66302.34(9)			

Note: Parameters of the ground states of CD_3 and CH_3 used in this work are adopted from Ref. [6] and [12], respectively.

state is now favored because of the nuclear spin statistics for the lower $^2A_1'$ vibronic state, indicating again the dominance of $K = 0$ levels for the vibrationally excited product. Qualitatively, the reactions yield a relatively cold rotational distribution for CH_3 and CD_3 products. As a consistent check of the vibronic assignment, taken our ν_0 (0_0^0) value and the 1081.7 cm^{-1} for $\nu_2' = 0 \rightarrow 1$ in the excited 3d $^2A'$ state, the observed position of $\delta_1(2_3^1)$ leads to an energy spacing of 1050.22 cm^{-1} for $\nu_2'' = 1 \rightarrow 3$ in the electronic ground state, which agrees very well with the more accurate literature value of 1050.218 cm^{-1}[5].

There is a peculiar dip near 66820 cm^{-1}, where the tunable ω_2 lies at 13301 cm^{-1}, in both CH_3 and CD_3 spectra shown in Figs.35. A closer examination revealed a nearly complete absence of VUV intensity in this region. An atomic Xe state of $5p^5 9s[3/2]_1^0$ lies at 93422 cm^{-1} above the ground state. We suspected that a double-resonant three-photon absorption and/or a resonance-enhanced sum-frequency mixing process ($2\omega_1 + \omega_2$) which yields a 93421 cm^{-1} radiation, occur in the VUV cell. Since at $\omega_2 \simeq 13301$ cm^{-1} both processes are double-resonant in nature, they compete very effectively with the desired difference-frequency mixing process, thus depleting the generation of the 66820 cm^{-1} radiation.

Let us now turn to the $\gamma_1(2_1^1)$ band. The electronic transition of the γ series is of $^2A_2'' \rightarrow {}^2E''$ in symmetry. The ν_2 vibration has an a_2'' symmetry in D_{3h} group. Hence, the $\gamma_1(2_1^1)$ vibronic band is of $^2A_1' \rightarrow {}^2E'$ in symmetry, i.e., a $\perp$-type transition. Although the band contour of CH_3 (Fig.3) seems consistent with this assignment with the central sharp peak at 67320 cm^{-1} being the Q-head for the $K = 0$ sub-band[19], its appearance for CD_3 (Fig.4) seems odd. The single-beam and the low energy crossed-beam data display a similar band contour as that for CH_3. The higher energy ones exhibit a very different contour with a three-peak feature. One plausible explanation is that in the electronically excited state, the ν_2 mode is Coriolis-coupled to a doubly degenerate ν_4 mode (an in-plane deformation mode with e' symmetry) which has a similar vibrational frequency as the ν_2 mode[18]. In addition, the vibrational level structures in the electronically excited state are conjectured to be such that the perturbation is stronger for the case of CD_3 than CH_3. This intermode Coriolis-coupling should be small for the low N states, but significantly enhanced with more rotational excitation, in particular for those levels with higher N and low K quantum numbers. Judging from the CD_3 $\delta_1(2_1^1)$ appearance in Fig.4 and 5, we anticipated that this Coriolis perturbation should manifest more clearly for the high energy collisions. Unfortunately, the broad spectral feature of the $\gamma_1(2_1^1)$ band, presumably from the fast predissociation nature, prevents us from any further analysis.

4 Summary

A (VUV + UV)-REMPI technique has been developed to detect the methyl radical. The spectroscopic properties of the electronically excited states were refined. More importantly, its sensitivity has been demonstrated to be sufficient high to allow the interrogation of this important radical possible even under the crossed-beam scattering conditions. In terms of the absolute sensitivity, it was estimated that a detection limit of $10^7/cm^3$ was achieved in this work. This estimation is based on the comparison with the analogous $F + H_2/D_2$ reactions and the better characterized (VUV + UV)-REMPI detection scheme for the H/D atoms[21]. The reported sensitivity is comparable to the more popular (2 + 1) or (3 + 1) REMPI detection scheme for this radical. In many of practical, diagnostic applications, such as in flame or CVD, the concentrations of the methyl radical are usually much higher. In those cases, the detection limitation is then not due to the signal strength, rather from the background or the spectral interference. Since the lasers were not focused in this work, very little background was encountered. Thus, the present (VUV + UV)-REMPI detection scheme could be a promising alternative from the S/N consideration. However, to make this detection scheme more valuable for reaction dynamics studies, further work is warranted, in particular about the relative predissociation rates of the intermediate states.

Works along this way are in progress.

Acknowledgments: This work is supported by the National Science Council of Taiwan. The assistance of Shih-Chieh Pu in experiments is acknowledged.

References

[1] Campbell I M. Energy and the Atmosphere, John Wiley & Sons. Ltd., London, 1977.

[2] Wayne R P. Chemistry of Atmospheres, Oxford University Press, Oxford, 2000.

[3] Jasinski J M, Meyerson B S, Scott B A. *Annu. Rev. Phys. Chem.*, 1987, **38**: 109

[4] Herzberg G. *Proc. Royal Soc., London*, 1961, A**262**: 291

[5] Fawzy W M, Sears T J, Davies P B. *J. Chem. Phys.*, 1990, **92**: 7021

[6] Sears T J, Frye J M, Spirko V, Kraemer W P. *J. Chem. Phys.*, 1989, **90**: 2125

[7] Hudgens J W, DiGiuseppe T G, Lin M C. *J. Chem. Phys.*, 1983, **79**: 571

[8] DiGiuseppe T G, Hudgens J W, Lin M C. *J. Phys. Chem.*, 1982, **86**: 36

[9] Parker D H, Wang Z W, Janssen M H M, Chandler D W. *J. Chem. Phys.*, 1989, **90**: 60

[10] Black J F, Powis I. *J. Chem. Phys.*, 1988, **89**: 3986

[11] Yamada C, Hirota E. *J. Chem. Phys.*, 1983, **78**: 669

[12] Yamada C, Hirota E, Kawaguchi K. *J. Chem. Phys.*, 1981, **75**: 5256

[13] Blush J A, Chen P, Wiedmann R T, White M G. *J. Chem. Phys.*, 1993, **98**: 3557

[14] Bacon J A, Pratt S T. *Chem. Phys. Lett.*, 1999, **311**: 346

[15] Westre S G, Kelly P B, Zhang Y P, Ziegler L D. *J. Chem. Phys.*, 1991, **94**: 270

[16] Botschwina P, Flesch J, Meyer W. *Chem. Phys.*, 1983, **74**: 321

[17] Velasco A M, Martin I, Lavin C. *Chem. Phys. Lett.*, 1997, **264**: 579

[18] Mebel A M R, Lin S H. *Chem. Phys.*, 1997, **215**: 329

[19] Ashfold M N, Clement S G, Howe J D, Western C M. *J. Chem. Soc. Faraday Trans.*, 1993, **89**: 1153

[20] Hsu Y T, Liu K, Pederson L A, Schatz G C. *J. Chem. Phys.*, 1999, **111**: 7921

[21] Dong F, Lee S H, Liu K. *J. Chem. Phys.*, 2000, **113**: 3633

[22] Skodje R T, Skouteris D, Manolopoulos D E, Lee S H, Dong F, Liu K. *J. Chem. Phys.*, 2000, **112**: 4536

[23] Hutchinson M H R, Thomas K J. *J. Quantum Electronics*, 1983, QE-**19**: 1823

[24] Herzberg. Molecular Spectra and Molecular Structure III. Electronic Spectra and Electronic Structure of Polyatomic Molecules, Princeton: Van Nostrand, 1966.

以(真空紫外光 + 紫外光)-共振加强式多光子游离法侦测交叉分子束之甲基生成物 *

郑伟良[a], **徐维成**, **周金刚**, **刘国平**[b]

(原子与分子科学研究所, 中央研究院, 信箱 23-166, 台北 106)

摘 要: 用(真空紫外光 + 紫外光)-共振加强式多光子游离法侦测甲基自由基.为证明此法之灵敏度,实验用交叉分子束反应 $F + CH_4(CD_4) \rightarrow HF(DF) + CH_3(CD_3)$,其绝对灵敏度可达 $10^7/cm^3$.由所得之光谱,更精确地得到两个里德堡态 $3d^2E''$及 $3d\ ^2A_1'$之光谱系数.

关键词: 四波混频;共振加强式多光子游离法;里德堡态;甲基

中图分类号: O64 **文献标识码**: A

* 楼南泉院士 80 华诞祝贺论文.

a. 太空科学研究所,中央大学,中坜,台北 106. b. 合聘教授,台湾大学化学系,台北 106, E-mail: kpliu@gate.sinica.edu.tw